Published in final edited form as:
Chem Sci. 2014 November ; 5(11): 4512–4516. doi:10.1039/C4SC01280A.

Peptide Targeting of Fluorescein-Based Sensors to Discrete Intracellular Locales

Robert J. Radford, **Wen Chyan**, and **Stephen J. Lippard**

Abstract

Fluorescein-based sensors are the most widely applied class of zinc probes but display adventitious localization in live cells. We present here a peptide-based localization strategy that affords precision in targeting of fluorescein-based zinc sensors. By appending the zinc-selective, reaction-based probe Zinpyr-1 diacetate (DA-ZP1) to the N-terminus of two different targeting peptides we achieve programmable localization and avoid unwanted sequestration within acidic vesicles. Furthermore, this approach can be generalized to other fluorescein-based sensors. When appended to a mitochondrial targeting peptide, the esterase-activated profluorophore 2′,7′-dichlorofluorescein diacetate can be used effectively at concentrations four-times lower than previously reported for analogous, non-acetylated derivatives. These results demonstrate on-resin or in-solution esterification of fluorescein to be an effective strategy to facilitate peptide-based targeting in live cells.

Introduction

Small-molecule fluorescent probes are important tools for investigating biology.[1] Among the most common scaffolds for optical probes are fluorescein derivatives because they are bright, non-toxic fluorophores that can be readily prepared on the gram scale.[2] Fluorescein derivatives, however, tend to be cell-impermeable and display adventitious cellular localization,[3] making it challenging to design probes that target discrete locales.

The failure to control cellular localization limits the utility of fluorescein-based probes. We have encountered this problem in our efforts to study the biology of mobile zinc. Mobile forms of zinc modulate numerous biological processes,[4] and families of zinc import, transport, and storage proteins tightly regulate the subcellular location and concentration of zinc ions.[5] The erratic cellular localization of most zinc probes, however, compromises their ability to delineate intracellular mobile zinc dynamics, causing confusion and controversy.[3a, 6] Zinpyr-1 (ZP1, Figure S1a), for example, readily enters live cells and accumulates primarily within the Golgi apparatus.[7] In contrast, a related sensor, Zinspy-5 (ZS5, Figure S1b), localizes to mitochondria in HeLa.[8] The ubiquitous Fluozin-3 (Figure

Correspondence to: Stephen J. Lippard.

[a]Department of Chemistry, Massachusetts Institute of Technology, 77 Massachusetts Avenue, Cambridge, MA 02139 Fax: 1-617-258-8150; Tel: 1-617-253-1892; E-mail: lippard@mit.edu

[†]Electronic Supplementary Information (ESI) available: Additional experiements, synthetic procedures, cell culturing protocols, and peptide characterization are provided. Fluorescence microscopy images were cropped for size, full-field views of all images are included in the Supplementary Information. See DOI: 10.1039/b000000x/

S1c) reportedly accumulates in the cytosol, vesicles, and Golgi apparati.[3b] Recent work with resorufin-based probes demonstrated that scaffolds other than fluorescein similarly suffer from unpredictable cellular localization,[9] highlighting the more general need for programmable delivery of optical probes.

To overcome the problem of adventitious localization of zinc sensors, our lab has invoked a peptide-based targeting strategy.[10] Peptides offer an unparalleled combination of chemical diversity, biocompatibility, and synthetic ease.[11] But we find that sequestration of fluorescein-labelled peptides within acidic vesicles presents an impediment that has prevented the adoption of peptide-based targeting by the wider chemical sensing community.

During the course of our studies we discovered a zinc-selective, reaction-based probe that effectively targets mitochondria in live cells (Figure S1d).[12] Our principal findings were (i) that installation of zinc-sensitive acetyl groups onto the phenolic oxygen atoms of a ZP1 derivative locked the fluorescein scaffold into its non-fluorescent lactone isomer; (ii) that the acetyl groups are stable to endogenous esterases but rapidly hydrolyze upon exposure to zinc, resulting in a significantly enhanced dynamic range;[12] and (iii) that acetylation also increased the hydrophobicity of the probe, thus enabling it to avoid endosomal entrapment and, instead, traffic to mitochondria via a triphenyl-phosphonium moiety.

In the current investigation, we applied these principles and evaluated peptide-based targeting motifs. Presented here are a series of peptide constructs featuring diacetylated Zinpyr-1 (DA-ZP1) attached to their N-terminii (Figure 1) which, to the best of our knowledge, thereby provide the first intracellular peptide-based zinc sensors. DA-ZP1-peptides are readily prepared in solution or on solid-phase and do not rely on endogenous esterases to unmask fluorescence. Instead, these probes undergo zinc-mediated ester hydrolysis, resulting in a zinc-selective and pH-insensitive fluorescence response. Through the combined contributions of targeting peptides and probe acetylation, DA-ZP1-peptides avoid endosomal sequestration and can effectively target the cytoplasm/nucleus, vesicles, or mitochondria. We further extend this two-pronged strategy to other fluorescein-based probes. When derivatized with a mitochondrial targeting peptide and phenolic acetyl groups, 2′,7′-dichlorofluorescein can effectively target mitochondria at bath concentrations four times lower than the reported literature value for a similar analogue.

Results and Discussion

Synthesis of Peptides with N-terminal Reaction-Based Probes

To establish the compatibility of DA-ZP1 with solid-phase peptide synthesis (SPPS), we created a three-residue, all alanine model peptide. Starting from Rink amide resin, Fmoc-protected alanine residues were sequentially added using standard procedures.[13] The (6-CO_2H) ZP1[14] probe was introduced onto the N-terminus of the peptide by developed methodology.[10] The resin was split into two portions; one portion was cleaved and purified by HPLC yielding the peptide ZP1-A_3. The second portion was allowed to react with a solution of acetic anhydride (50 %, v/v) in dimethylformamide (DMF) for 5 h. The resin was then washed with DMF and dichloromethane, dried, and cleaved in mixture of

triisopropylsilane (5%, v/v) in trifluoroacetic acid. The overall yield for the synthesis of DA-ZP1-A_3 was estimated to be 44% by analytical HPLC.

As a parallel strategy, acetyl groups were installed onto ZP1-peptide derivatives by stirring the purified ZP1-labelled peptide in a mixture of acetic anhydride in dimethyl sulfoxide (DMSO) at room temperature for ≥ 4 h (see Supplementary Information for details). Under our reaction conditions, moderate to excellent yields (52-98%) were obtained. Using these synthetic routes, we synthesized DA-ZP1-R_9, DA-ZP1-r(F_xr)$_3$, DA-DCF-r(F_xr)$_3$, as well as their non-acetylated analogues. The successful synthesis and purification of these constructs demonstrates our reaction-based probes are compatible with the cleavage and purification conditions of SPPS and zinc-reactive acetyl groups can be incorporated onto ZP1-labelled peptides with moderate to excellent yields.

DA-ZP1-Peptides have Large Dynamic Ranges, are Selective for Zn(II), and pH Insensitive

Using DA-ZP1-A_3 as a model system, we assessed its photophysical and zinc-binding properties (Figure 2). DA-ZP1-A_3 is spectroscopically silent at λ_{abs} > 350 nm and essentially non-fluorescent (Φ < 0.001). Addition of excess $ZnCl_2$ rapidly restores ($t_{½}$ = 0.053 ± 0.008 min) the absorption ($\lambda_{abs, Zn}$ = 509 nm) and emission ($\lambda_{em, Zn}$ = 530 nm; Φ_{Zn} = 0.80 ± 0.03) bands associated with 2′,7′-dichlorofluorescein. Removing zinc ions from the sensor with ethylenediaminetetraacetic acid (EDTA) yields ZP1-A_3, which has photophysical and zinc-binding properties similar to those of other Zinpyr sensors (λ_{abs} = 519 nm; λ_{em} = 538 nm; Φ_{Zn} = 0.14 ± 0.01; $K_{d\text{-}Zn}$ = 0.38 ± 0.04 nM) (Table S1).[2d] Relevant properties and attributes for acetylated and non-acetylated ZP1-labelled peptides are given in the Supplemental Information (Figures S2-S7 and Tables S1-S2). Spectroscopic and zinc-binding properties of all constructs were in accord with expectations,[2d] although we note a small redshift in the absorption and emission maxima when the sensor is attached to the R_9 and r(F_xr)$_3$ peptides.

In contrast to the non-acetylated ZP1-A_3, DA-ZP1-A_3 does not show any significant turn-on under acidic conditions (Figure 3d). Traditional Zinpyr sensors rely solely on photoinduced electron transfer (PET) from nitrogen-rich zinc-binding units to quench the metal-free form of the probe.[2d] Nitrogen donors provide selectivity for zinc over biologically abundant metal ions such as calcium and magnesium but they also render Zinpyr sensors pH sensitive.[15] By forcing the fluorescein scaffold into the non-fluorescent lactone isomer, the zinc-reactive acetyl groups introduce an additional quenching mechanism and minimize unwanted proton induced turn-on.

Peptide Vectors Target ZP1 to the Cytoplasm/Nucleus, Vesicles, or Mitochondria

For an initial targeting vector, we chose a nona-arginine (R_9) internalization sequence. This sequence, which has been extensively studied, delivers various cargos, including fluorescein, to the cytoplasm and nucleus.[11b, 16] When HeLa cells were pretreated with 5 μM ZP1-R_9, a punctate pattern was observed throughout the cytoplasm, which co-localized moderately with endosomal tracker Lysotracker Red, Pearson's r = 0.42 ± 0.16 (Figure 3, a-d).[17‡] Bathing cells in medium containing a zinc ionophore, zinc pyrithione (ZnPT, 25 μM), resulted in no significant increase in the fluorescence signal (data not shown). The loss of

zinc response in ZP1-R_9 is attributed to sequestration of the probe within acidic, endocytotic vesicles. These results mirror recent work with ZP1-TPP, which revealed the propensity for ZP1 conjugates to accumulate within acidic vesicles and lose their ability to respond to zinc.[12]

The reaction-based probe DA-ZP1-R_9, in contrast, was distributed throughout the cytoplasm and nucleus (Figure 4, e-h). When cells pretreated with 2.5 μM DA-ZP1-R_9 were bathed in medium supplemented with 25 μM ZnPT, an approximate 3.5-fold increase in the normalized intracellular fluorescence signal was observed (Figure 4). Addition of the intracellular chelator *N*,*N*,*N*′,*N*′-tetrakis(2-pyridylmethyl)ethylenediamine (TPEN, 50 μM) partially attenuated the fluorescence signal, presumably by removing zinc from the sensor and restoring the ability of the dipicolylamine arms to quench fluorescence via PET. Because zinc-mediated ester hydrolysis is irreversible, however, the signal cannot return to initial levels.

When HeLa cells were pretreated with medium containing 1 μM DA-ZP1-R_9, the sensor localized to vesicles (Figure 5). These results are consistent with an energy-dependent uptake mechanism such as endocytosis.[18] Further support for such a mechanism is the inability of DA-ZP1-R_9 to penetrate the plasma membrane when incubated with live cells at 4 °C (Figure S8). Because the fluorescence turn-on of DA-ZP1-R_9 is pH-insensitive, however, the probe was still able to detect an influx of zinc within vesicles (Figure 6). We note, however, that once the acetyl groups are removed the resulting construct, ZP1-R_9, is susceptible to proton-induced turn-on. Thus, addition of TPEN did not attenuate the fluorescence signal (Figure 6). Nevertheless, these results demonstrate that peptides can be used to direct zinc sensors to vesicles, which are important targets in metalloneurochemistry.[19]

To investigate additional peptide constructs, we prepared mitochondrial-targeting DA-ZP1-r(F_xr)$_3$. First reported by the Kelley lab,[11b,20] the mitochondrial-penetrating peptide, (F_xr)$_3$, is composed of non-natural amino acids L-cyclohexylalanine (F_x) and D-arginine and can deliver chemotherapeutics and small-molecule fluorophores specifically to mitochondria in live cells.[11b,20] As was the case for ZP1-R_9, the non-acetylated derivative, ZP1-(F_xr)$_3$, was sequestered within acidic vesicles (Figure 7, a-d) and failed to respond to zinc. We therefore prepared another construct, ZP1-r(F_xr)$_3$, featuring an additional N-terminal arginine to aid in mitochondrial targeting by mitigating the negative charge of the 2-carboxylate group on fluorescein.[20b] ZP1-r(F_xr)$_3$, however, also failed to deliver ZP1 to mitochondria (data not shown). In contrast, DA-ZP1-r(F_xr)$_3$ localized moderately to mitochondria at concentrations as low as 1 μM (Pearson's r = 0.41 ± 0.09) (Figure 7e-f). We speculate that the lower Pearson's value is due to some portion of the construct being sequestered within acidic vesicles. Consistent with this hypothesis is the observation that DA-ZP1-r(F_xr)$_3$ enters cells by an energy-dependent mechanism (Figure S9).

DA-ZP1-r(F_xr)$_3$ detects changes in mobile zinc concentration within mitochondria. When HeLa cells were pretreated with 1 μM DA-ZP1-r(F_xr)$_3$ and bathed in medium containing 25

‡We adopted the nomenclature set in ref. 24 to describe the extent of co-localization between labelled peptides and organelle trackers.

μM ZnPT, a 10-fold increase in fluorescence was observed (Figure 8). Addition of TPEN (50 μM) reduced the fluorescence signal, validating the zinc-dependent nature of the response (Figure 8).

These results with DA-ZP1-R_9 and DA-ZP1-r$(F_x r)_3$ demonstrate that our reaction-based probes generally avoid endosomal sequestration. Although, in contrast to DA-ZP1-TPP, esterases can slowly hydrolyse the DA-ZP1-peptide constructs in vitro (Figure S10), within a live cell environment, DA-ZP1 in combination with a localizing peptide sequence can direct fluorescein-based zinc probes to discrete cellular locales.

Peptide-based Targeting of the Esterase-sensitive 2′,7′-Dichlorofluorescein Diacetate

Given the prevalence of fluorescein-labelled peptides in biological studies and the dramatic difference in localization between acetylated versus non-acetylated ZP1-peptides, we investigated whether acetylation could improve the uptake and localization of a 2′,7′-dichlorofluorescein labelled peptide. Fluorescein constructs are commonly used as fluorescent tags in order to visualize the localization of peptide constructs within live cells. Recent literature, however, reveals that fluorescein is a “non-innocent” reporter that can alter the uptake and localization of a peptide.[18a,21] Achieving significant uptake of fluorescein-labelled peptides often requires high loading concentrations of ≥ 10 μM, co-administration with endosomal disrupting agents, or modification of sidechain residues.[18a,20b,22] Using r$(F_x r)_3$ as a model system, we compared the uptake and localization of peptide derivatives labelled with 2′,7′-dichlorofluorescein (DCF) or 2′,7′-dichlorofluorescein diacetate (DA-DCF), respectively. DA-DCF relies on endogenous esterases to remove the acetyl groups and restore the fluorescent properties of the probe (Figure S11).[1] At a concentration of 5 μM, DCF-r$(F_x r)_3$ failed to significantly penetrate the plasma membrane (Figure 9a-c). DA-DCF-r$(F_x r)_3$, in contrast, permeated the plasma membrane and localized within mitochondria. The co-localization between MitoTracker Red and DA-DCF-r$(F_x r)_3$ yielded Pearson's $r = 0.57 \pm 0.16$. A heterogeneous population distribution was observed, with some cells failing to accumulate appreciable quantities of peptide (Figure 9e, blue outline). For completeness, all cells, regardless of signal intensity, were included in the co-localization calculation. Cells with appreciable emission intensity had a significantly higher localization correlation, Pearson's $r = 0.83 \pm 0.08$ (Figure 9e, red outline). The reason for the heterogeneous distribution is unknown. Nonetheless, this proof-of-concept study shows that modification of the fluorescein provides a facile strategy to overcome altered localization of targeting peptides by an appended fluorophore. Because fluorescein diacetate has stability issues when incubated in complete medium,[23] however, modification of the fluorescein with the acetoxymethyl ester group may provide a more robust platform for peptide targeting in live slice and animal studies.[23]

Conclusion

Zinpyr-1 diacetate (DA-ZP1) has been successfully incorporated into peptide scaffolds using SPPS methodologies. With the use of peptides as modular targeting vectors, ZP1 was directed in a programmed manner to the cytoplasm/nucleus, vesicles, or mitochondria in live HeLa cells and responded to changes in intracellular mobile zinc concentration. By

overcoming the adventitious localization of small-molecule zinc sensors, peptide-based targeting provides a valuable complement to existing small-molecule sensors aimed at understanding the bioinorganic chemistry of mobile zinc. Moreover, acetylating a 2′-7′ dichlorofluorescein derivative enabled peptide targeting of mitochondria at concentrations four times lower than the reported literature value for a similar, non-acetylated derivative.[20b] These results indicate that acetylation of fluorescein-labelled peptides is an effective strategy for preventing fluorescein from altering the cellular locale of peptide constructs. With the ability to direct sensors effectively in live cells, peptide-based targeting could be extended to fluorescein-based sensors that detect biological analytes besides zinc, such as reactive oxygen and nitrogen species, enzymes, and other metal ions.

Supplementary Material

Refer to Web version on PubMed Central for supplementary material.

Acknowledgments

This work was supported by NIH grant GM065519 from the National Institute of General Medical Sciences.

Notes and references

1. Johnson, I.; Spence, MTZ. The Molecular Probes Handbook. 11. 2010.
2. (a) Rossi FM, Kao JPY. Bioconjugate Chem. 1997; 8:495–497.(b) Sun WC, Gee KR, Klaubert DH, Haugland RP. J Org Chem. 1997; 62:6469–6475.(c) Jiang PJ, Guo Z. Coord Chem Rev. 2004; 248:205–229.(d) Nolan EM, Lippard SJ. Acc Chem Res. 2009; 42:193–203. [PubMed: 18989940] (e) Chang PV, Bertozzi CR. Chem Commun (Camb). 2012; 48:8864–8879. [PubMed: 22801420]
3. (a) Kay AR, Rumschik SM. Metallomics. 2011; 3:829–837. [PubMed: 21681308] (b) Qin Y, Miranda JG, Stoddard CI, Dean KM, Galati DF, Palmer AE. ACS Chem Biol. 2013; 8:2366–2371. [PubMed: 23992616]
4. Pluth MD, Tomat E, Lippard SJ. Annu Rev Biochem. 2011; 80:333–355. [PubMed: 21675918]
5. (a) Huang L, Tepaamorndech S. Mol Aspects Med. 2013; 34:548–560. [PubMed: 23506888] (b) Jeong J, Eide DJ. Mol Aspects Med. 2013; 34:612–619. [PubMed: 23506894]
6. Kay AR. Trends Neurosci. 2006; 29:200–206. [PubMed: 16515810]
7. Walkup GK, Burdette SC, Lippard SJ, Tsien RY. J Am Chem Soc. 2000; 122:5644–5645.
8. Nolan EM, Ryu JW, Jaworski J, Feazell RP, Sheng M, Lippard SJ. J Am Chem Soc. 2006; 128:15517–15528. [PubMed: 17132019]
9. Loas A, Radford RJ, Lippard SJ. Inorg Chem. 2014
10. Radford RJ, Chyan W, Lippard SJ. Chem Sci. 2013; 4:3080–3084. [PubMed: 23878718]
11. (a) Kratz F, Müller IA, Ryppa C, Warnecke A. ChemMedChem. 2008; 3:20–53. [PubMed: 17963208] (b) Stewart KM, Horton KL, Kelley SO. Org Biomol Chem. 2008; 6:2242–2255. [PubMed: 18563254] (c) Li L, Ge J, Wu H, Xu QH, Yao SQ. J Am Chem Soc. 2012; 134:12157–12167. [PubMed: 22734946]
12. Chyan W, Zhang DY, Lippard SJ, Radford RJ. Proc Natl Acad Sci USA. 2014; 111:143–148. [PubMed: 24335702]
13. Kirin SI, Noor F, Metzler-Nolte N, Mier W. J Chem Educ. 2007; 84:108–111.
14. Woodroofe CC, Masalha R, Barnes KR, Frederickson CJ, Lippard SJ. Chem Biol. 2004; 11:1659–1666. [PubMed: 15610850]
15. Wong BA, Friedle S, Lippard SJ. J Am Chem Soc. 2009; 131:7142–7152. [PubMed: 19405465]
16. Fischer R, Köhler K, Fotin-Mleczek M, Brock R. J Biol Chem. 2004; 279:12625–12635. [PubMed: 14707144]
17. Zinchuk V, Wu Y, Grossenbacher-Zinchuk O. Sci Rep. 2013; 3

18. (a) Jones AT, Sayers EJ. J Control Release. 2012; 161:582–591. [PubMed: 22516088] (b) Stanzl EG, Trantow BM, Vargas JR, Wender PA. Acc Chem Res. 2013; 46:2944–2954. [PubMed: 23697862]

19. Radford RJ, Lippard SJ. Curr Opin Chem Biol. 2013; 17:129–136. [PubMed: 23478014]

20. (a) Horton KL, Stewart KM, Fonseca SB, Guo Q, Kelley SO. Chem Biol. 2008; 15:375–382. [PubMed: 18420144] (b) Yousif LF, Stewart KM, Horton KL, Kelley SO. ChemBioChem. 2009; 10:2081–2088. [PubMed: 19670199] (c) Wisnovsky SP, Wilson JJ, Radford RJ, Pereira MP, Chan MR, Laposa RR, Lippard SJ, Kelley SO. Chem Biol. 2013; 20:1323–1328. [PubMed: 24183971]

21. (a) Fischer R, Waizenegger T, Köhler K, Brock R. Biochimica Et Biophysica Acta-Biomembranes. 2002; 1564:365–374.(b) Puckett CA, Barton JK. J Am Chem Soc. 2009; 131:8738–8739. [PubMed: 19505141]

22. (a) Carrigan CN, Imperiali B. Anal Biochem. 2005; 341:290–298. [PubMed: 15907875] (b) El-Sayed A, Futaki S, Harashima H. AAPS J. 2009; 11:13–22. [PubMed: 19125334]

23. Lavis LD, Chao TY, Raines RT. Chem Sci. 2011; 2:521–530. [PubMed: 21394227]

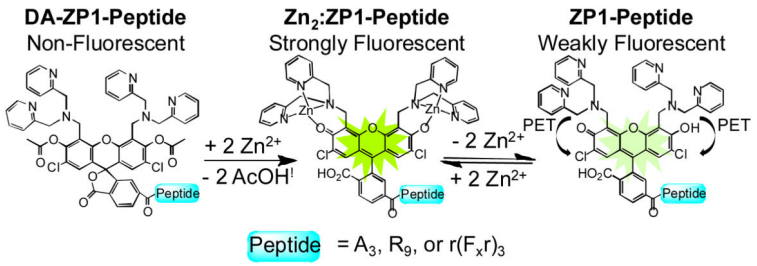

Fig. 1.

Scheme illustrating the two zinc-sensing mechanisms operating within peptide constructs. Charge and water molecules omitted for clarity.

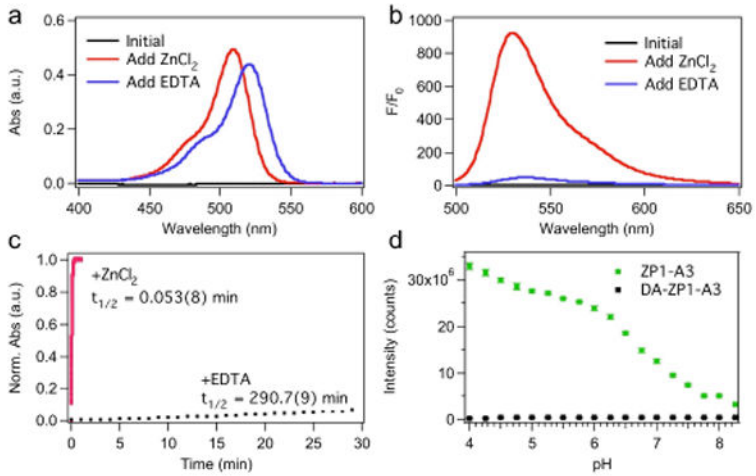

Fig. 2.

In vitro characterization of DA-ZP1-A_3. (a) UV-vis and (b) fluorescence spectra of a 5-μM solution of DA-ZP1-A_3 in buffer (50 mM PIPES, 100 mM KCl; pH 7). Spectra were acquired initially (black line), upon addition of 100 μM $ZnCl_2$ (red line), and again after addition of 200 μM EDTA (blue line). (c) Time-dependent change in the normalized absorbance of a ca. 5-μM solution DA-ZP1-A_3 at 37 °C in buffer (50 mM PIPES, 100 mM KCl; pH 7) in the presence of 100 μM $ZnCl_2$ (red squares, λ_{abs} = 510 nm) or EDTA (black squares, λ_{abs} = 520 nm). (d) Integrated fluorescence intensity of a 1-μM solution of ZP1-A_3 (green circles) or DA-ZP1-A_3 (black squares) as a function of pH. See Supplemental Information for experimental details.

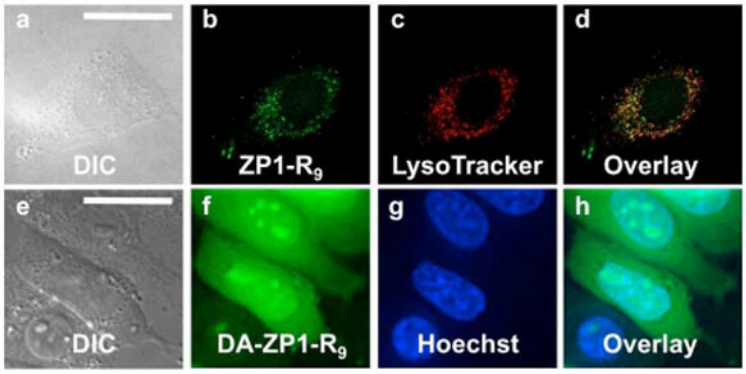

Fig. 3.

Deconvoluted fluorescence microscopy images of live HeLa cells pretreated with ZP1-R_9 (5 μM) or DA-ZP1-R_9 (2.5 μM) and the indicated organelle stain. Top, ZP1-R_9: (a) Differential interference contrast (DIC) image, (b) signal from ZP1-R_9, (c) signal from LysoTracker Red, (d) overlay of (b) and (c). Pearson's $r = 0.42 \pm 0.16$ (n = 8). Bottom, DA-ZP1-R_9: (e) DIC, (f) signal from DA-ZP1-R_9 after treatment with 25 μM ZnPT, (g) signal from Hoechst 33258, (h) overlay of (f) and (g). Scale bar = 25μm

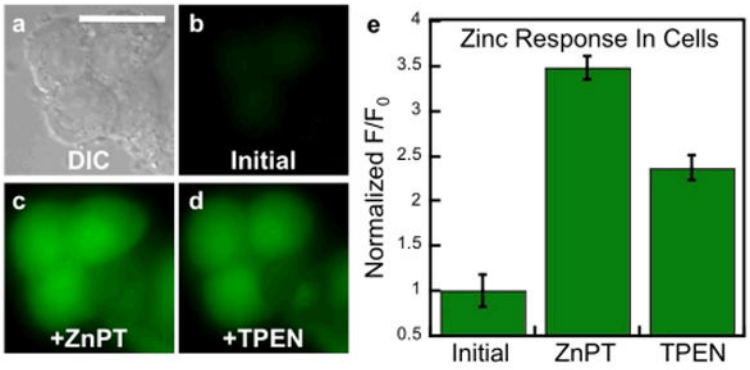

Fig. 4.

Response of DA-ZP1-R_9 to zinc pyrithione (ZnPT) in live HeLa cells. (a) DIC image. Signal from DA-ZP1-R_9 (b) initially, (c) after addition 25 μM ZnPT, and (d) after addition of 50 μM TPEN. (e) Normalized fluorescence response in live cells. Scale bar = 25 μm

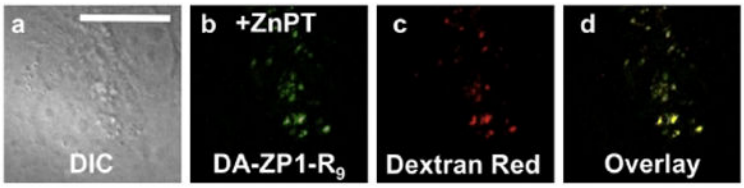

Fig. 5.

Deconvoluted fluorescence microscopy images of live HeLa cells pretreated with 1 μM DA-ZP1-R_9 and 100 nM Dextran Red. (a) DIC image. (b) Signal from DA-ZP1-R_9 after addition of 25 μM ZnPT (c) signal from Dextran Red, (d) overlay of (b) and (c). Pearson's $r = 0.55 \pm 0.12$ (n = 11). Scale bar = 25 μm

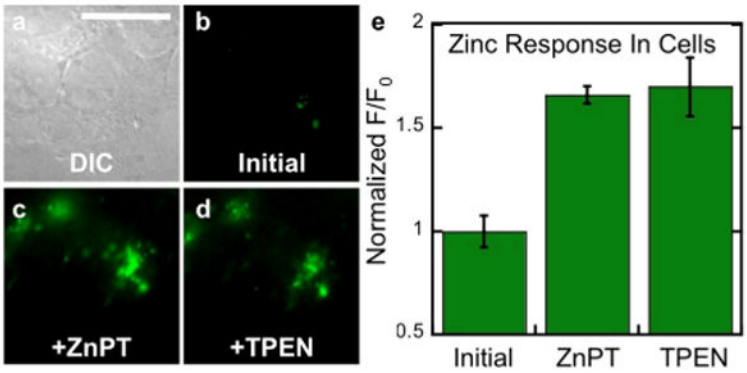

Fig. 6.

Fluorescence microscopy of live HeLa cells pretreated with 1 μM DA-ZP1-R_9. (a) DIC image. Signal from DA-ZP1-R_9 (b) initially, (c) after addition of 25 μM ZnPT, and (d) after addition of 50 μM TPEN. (e) Quantification of the zinc-induced fluorescence response. Scale bar = 25 μm

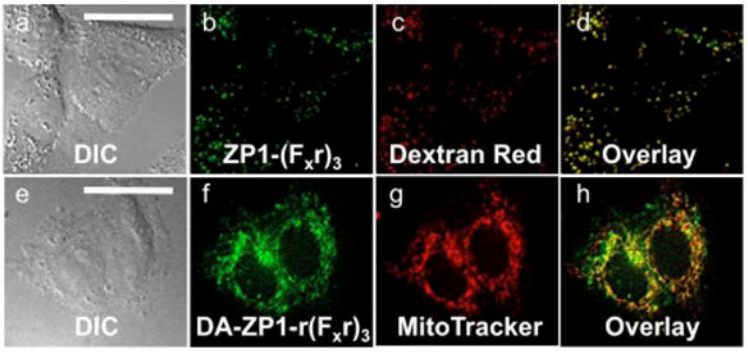

Fig. 7.

Deconvoluted fluorescence microscopy images of ZP1-$(F_xr)_3$ and DA-ZP1-r$(F_xr)_3$ in live HeLa cells. Top, cells pretreated with medium containing 2.5 μM of ZP1-$(F_xr)_3$: (a) DIC image, (b) signal from ZP1-$(F_xr)_3$, (c) signal from Dextran Red, (d) overlay of (b) and (c). Pearson's $r = 0.71 \pm 0.07$. Bottom, cells pretreated with 1 μM DA-ZP1-r$(F_xr)_3$: (e) DIC, (f) signal from DA-ZP1-r$(F_x)_3$ after treatment with 25 μM ZnPT, (g) signal from MitoTracker Red, (h) overlay of (f) and (g). Pearson's $r = 0.41 \pm 0.09$. Scale bar = 25 μm

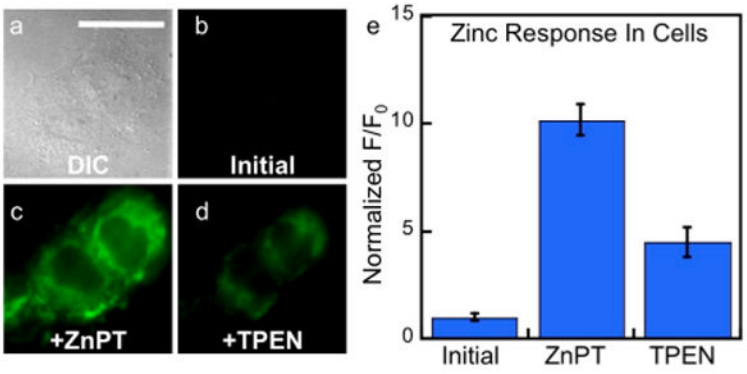

Fig. 8.

Response of DA-ZP1-r(F_xr)$_3$ to zinc pyrithione in live HeLa cells. (a) Differential contrast image (DIC). Signal from ZP1-R_9 (b) initially, (c) after addition 25 μM ZnPT, and (d) after addition of 50 μM TPEN. (e) Quantification of the fluorescence response in live HeLa cells normalized to initial level (n = 9). Scale bar = 25 μm

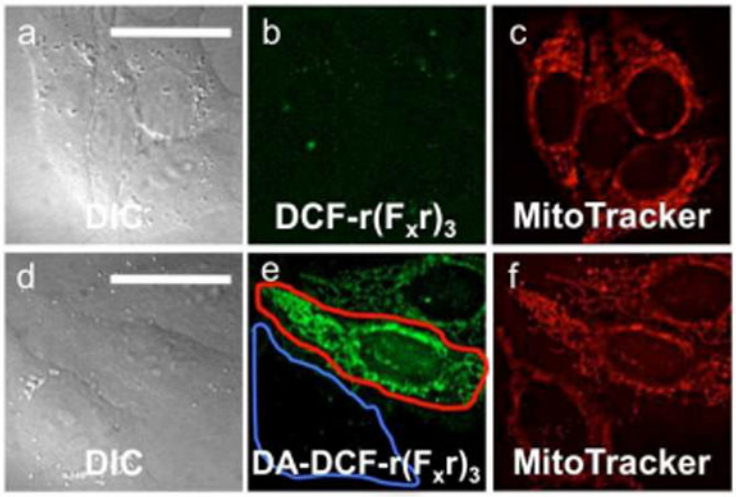

Fig. 9.

Deconvoluted fluorescence microscopy images of DCF-r(F_xr)$_3$ and DA-DCF-r(F_xr)$_3$ in live HeLa cells. Top, cells pretreated with 5 μM DCF-r(F_xr)$_3$ and 500 nM MitoTracker Red for 30 min. (a) differential contrast image (DIC), (b) signal from DCF-r(F_xr)$_3$, (c) signal from MitoTracker Red. Bottom, cells pretreated with 5 μM DA-DCF-r(F_xr)$_3$ and 500 nM MitoTracker Red for 30 min. (d) DIC, (e) signal from DCF-r(F_xr)$_3$, (f) signal from MitoTracker Red. The global Pearson's r = 0.57 ± 0.16 (n = 37). Cells with high levels of DA-DCF-r(F_xr)$_3$ (e, red outline) have a higher Pearson's r = 0.83 ± 0.08 (n = 10). Scale bar = 25 μm